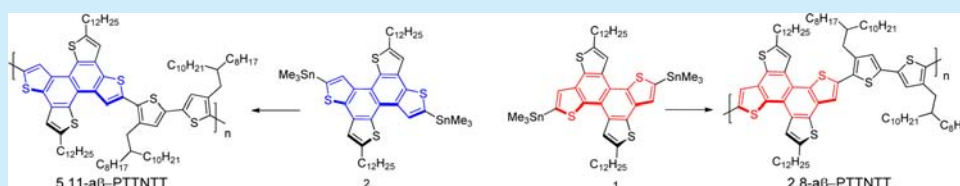


## Synthesis and Molecular Properties of Two Isomeric Dialkylated Tetrathienonaphthalenes

Shao-Ling Chang,<sup>‡</sup> Chih-Wen Lu,<sup>‡</sup> Yu-Ying Lai, Jhih-Yang Hsu, and Yen-Ju Cheng\*

Department of Applied Chemistry, National Chiao Tung University, 1001 University Road, Hsin-Chu, Taiwan

## Supporting Information

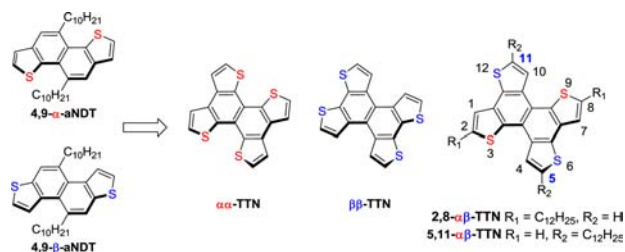


**ABSTRACT:** Isomeric 2,8-distannyl 5,11-didodecyl  $\alpha\beta$ -TTN (1, tetrathienonaphthalene = TTN) and 2,8-didodecyl 5,11-distannyl  $\alpha\beta$ -TTN (2) have been designed and successfully synthesized. The naphthalene core structures in  $\alpha\beta$ -TTNs were constructed by a systematic protocol using  $\text{PtCl}_2$ -catalyzed cyclization followed by oxidative Scholl annulation in good yields. Compared to the one-dimensional naphthodithiophene derivatives, the two-dimensional  $\alpha\beta$ -TTN molecules showed good solubility, extended conjugation, strong absorptivity, and highly coplanar structures. Compounds 1 and 2 were polymerized with a 5,5'-dibromo-2,2'-bithiophene-based monomer to afford 2,8- $\alpha\beta$ -PTTNTT and 5,11- $\alpha\beta$ -PTTNTT copolymers. 2,8- $\alpha\beta$ -PTTNTT with the  $\alpha$ -aNDT moiety in the main chain exhibited a higher hole mobility of  $1.26 \times 10^{-2} \text{ cm}^2 \text{ V}^{-1} \text{ s}^{-1}$ .

Coplanar acenedithiophene (AcDT) derivatives have been superior building blocks for the creation of various organic semiconductors due to their facile functionalization and high charge mobility.<sup>1</sup> For example, benzodithiophene (BDT)-incorporating donor–acceptor (D–A) copolymers represent the most successful materials to achieve high-efficiency solar cells,<sup>2</sup> while anthradithiophene-based (ADT) materials have been demonstrated to exhibit high mobilities for organic field-effect transistors.<sup>3</sup> Naphthodithiophenes (NDT) with a size in between BDT and ADT in the AcDT family have also attracted considerable research interest in terms of their versatile structures and prominent properties.<sup>4</sup> Depending on the fused junction between the thiophene and naphthalene moieties, NDT generally can have linear- and angular-shaped isomeric structures. Angular-shaped NDTs (aNDTs) can be further divided into  $\alpha$ -aNDT and  $\beta$ -aNDT isomers (see Scheme 1). To fully exploit these NDT-based materials for solution-processable organic electronics, incorporation of aliphatic groups on the bare NDTs is essential in order to ensure the solubility as well as to

induce favorable intermolecular interactions.<sup>5</sup> We have recently reported a systematic method to regiospecifically substitute two alkyl groups at 4,9- or 5,10-positions of the  $\alpha$ -aNDT and  $\beta$ -aNDT, forming four isomeric dialkylated NDT structures.<sup>6</sup> Takimiya and Osaka et al. demonstrated that the molecular geometry of the isomeric NDT structures plays a key role in governing the molecular packing and structure ordering, which ultimately determines the device performance.<sup>7</sup> Specifically, D–A copolymers using the angular-shaped 4,9- and 5,10-dialkylated  $\alpha$ -aNDT units with relatively linear polymer backbones have shown superb solar cell performance.<sup>8</sup> Extending a linear conjugation along its vertical direction to form a two-dimensional conjugated system is a rational design to enhance  $\pi$ – $\pi$  interaction and absorption ability.<sup>9</sup> Employing such molecular engineering has successfully led to high-performance polymer solar cells.<sup>10</sup> It is, therefore, of great interest to further extend the  $\pi$ -conjugation on the basis of an aNDT core. By fusing two more thiophene units on the 4,5- and 9,10-junctions of a horizontally aligned aNDT unit, a new two-dimensional tetrathienonaphthalene (TTN) structure embedding another vertically aligned aNDT will be generated. The cruciform-shaped TTN family can generally have three isomeric structures depending on the relative placement of the thienyl rings on the central naphthalene core. If two  $\alpha$ -aNDTs or two  $\beta$ -aNDTs merge together, we denote them as  $\alpha\alpha$ -TTN<sup>11</sup> and  $\beta\beta$ -TTN,<sup>12</sup> respectively (Scheme 1). Similarly,  $\alpha\beta$ -TTN is composed of an  $\alpha$ -NDT and a  $\beta$ -NDT that share the central naphthalene core. Yamaguchi et al. have reported the synthesis of  $\alpha\alpha$ -TTN derivatives in which the four sulfur atoms point at the fjord region.<sup>11d</sup> To the best of our

Scheme 1. Chemical Structures of aNDT and TTN Derivatives

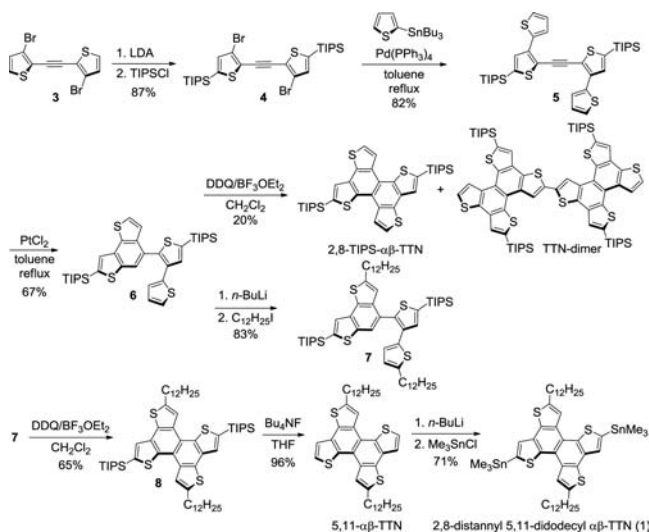


Received: November 16, 2015

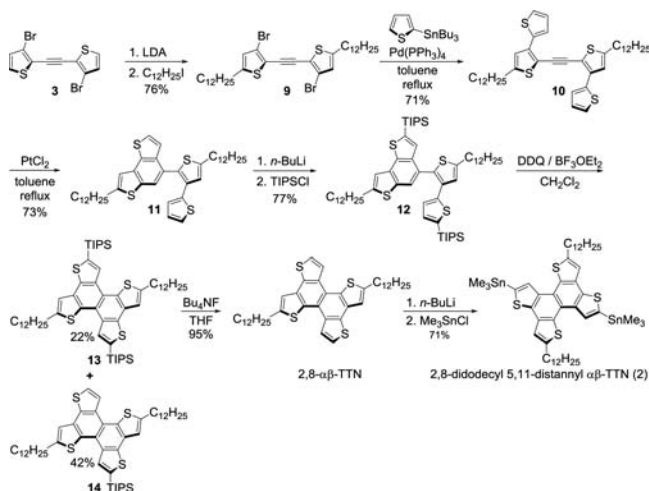
Published: January 7, 2016

knowledge, however,  $\alpha\beta$ -TTN derivatives have never been synthesized. The structural feature of the  $\alpha\beta$ -TTN structure is that the four sulfur atoms in the thiophene rings are positioned in a head-to-tail arrangement circling around the central naphthalene core. It is desirable to incorporate the two-dimensional  $\alpha\beta$ -TTN units into the conjugated copolymers. In this research, we design a new synthetic strategy to introduce two dodecyl groups at the  $\beta$ -aNDT or  $\alpha$ -aNDT moieties in a  $\alpha\beta$ -TTN, resulting in two isomeric structures denoted as 5,11- $\alpha\beta$ -TTN and 2,8- $\alpha\beta$ -TTN respectively (Scheme 1). These two isomers are selectively distannylated to form 2,8-distannyl 5,11-didodecyl  $\alpha\beta$ -TTN (1) and 2,8-didodecyl 5,11-distannyl  $\alpha\beta$ -TTN (2) (Schemes 2 and 3) which can be used for future  $\pi$ -extension or

### Scheme 2. Synthetic Route toward 2,8-Distannyl 5,11-Didodecyl $\alpha\beta$ -TTN (1)



### Scheme 3. Synthetic Route toward 2,8-Didodecyl 5,11-Distannyl $\alpha\beta$ -TTN (2)



polymerization. It is envisaged that the structural geometry and electronic orbital of the two isomeric  $\alpha\beta$ -TTN moieties will play an important role in achieving high-performance materials.

A well-designed synthetic route to make compound 1 is developed and is shown in Scheme 2. The compound 3 was lithiated by lithium diisopropylamide (LDA) followed by reacting with triisopropylsilyl chloride (TIPSCl) to obtain the

disilylated product 4.<sup>13</sup> Stille coupling reaction of compound 4 with 2-(tributylstannyl) thiophene afforded compound 5.  $\text{PtCl}_2$ -catalyzed intramolecular cyclization of the diene-yne moiety in compound 5 afforded compound 6 in 67% yield. The X-ray single crystal structure of 6 shown in the Figure 1 verifies that the

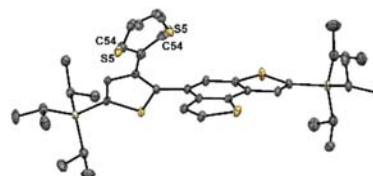
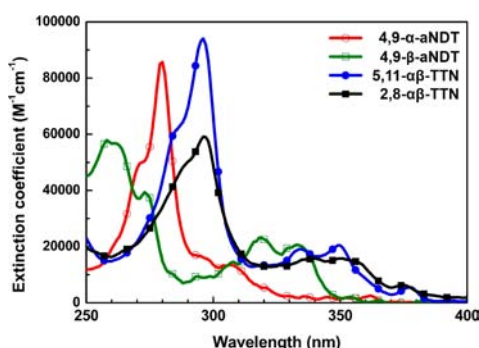


Figure 1. X-ray single crystal structure of 6 (50% probability for thermal ellipsoids). S<sup>5</sup> and C<sup>54</sup> are interchangeable due to the structural disorder.

cyclization is indeed via a 6-endo-dig rather than a 5-exo-dig fashion.<sup>14</sup> Scholl-type oxidative cyclization of compound 6 with 2,3-dichloro-5,6-dicyano-1,4-benzoquinone (DDQ)/ $\text{BF}_3\text{OEt}_2$  successfully led to the desired 2,8-TIPS- $\alpha\beta$ -TTN product which was also confirmed by its X-ray crystallography, and is shown in Figure S1. However, the product was swiftly converted to the dimer and oligomers resulting from intermolecular oxidative coupling between the unprotected 5,11-positions of 2,8-TIPS- $\alpha\beta$ -TTN. To prevent this side reaction, the  $\alpha$ -hydrogen of the thiophenes in compound 6 was deprotonated by  $n\text{-BuLi}$  followed by the nucleophilic substitution with 1-iodododecane to form the didodecyl compound 7. Under the DDQ/ $\text{BF}_3\text{OEt}_2$  condition, the protected 7 successfully underwent Scholl cyclization to furnish the desired compound 8 in 65% yield. It should be emphasized that using dry and degassed dichloromethane is the key to succeeding in this reaction which is generally considered as a cation-radical mechanism.<sup>15</sup> Desilylation of compound 8 by tetrabutyl ammonium fluoride (TBAF) formed 5,11- $\alpha\beta$ -TTN which was subsequently distannylated to accomplish the target compound 1 (2,8-distannyl 5,11-didodecyl  $\alpha\beta$ -TTN). By adopting a similar strategy, the synthesis of another isomeric counterpart 2 is shown in Scheme 3. The thiophene rings in compound 3 were functionalized with two dodecyl groups to form compound 9. Palladium-catalyzed Stille coupling of compound 9 with 2-(tributylstannyl)thiophene generated compound 10.  $\text{PtCl}_2$ -catalyzed 6 $\pi$ -cyclization of 10 formed compound 11. Again, the two thiophene rings in compound 11 were protected by the TIPS groups to form compound 12 followed by the DDQ/ $\text{BF}_3\text{OEt}_2$ -oxidative annulation to obtain  $\alpha\beta$ -TTN 13. The one-side desilylated compound 14 was also obtained. Without further purification, the mixture of compound 13 and 14 was desilylated by TBAF to obtain the single 2,8- $\alpha\beta$ -TTN product which was distannylated to furnish the 2,8-didodecyl 5,11-distannyl  $\alpha\beta$ -TTN (2).

The absorption spectra of two isomeric  $\alpha\beta$ -TTNs along with 4,9- $\alpha$ -aNDT and 4,9- $\beta$ -aNDT are shown in Figure 2, and the parameters are shown in Table 1.<sup>6</sup> The profiles of the absorption spectra of the two isomeric structures are essentially the same. However, the 5,11- $\alpha\beta$ -TTN showed much stronger extinction coefficients from 260 to 310 nm than the corresponding 2,8- $\alpha\beta$ -TTN. It should be noted that compared to the one-dimensional 4,9- $\alpha$ -aNDT and 4,9- $\beta$ -aNDT molecules, the two-dimensional  $\alpha\beta$ -TTN exhibited significant red-shifting in the absorption bands, indicating that merging two aNDT molecules in the  $\alpha\beta$ -TTN results in the extension of conjugation through orbital interactions. The electrochemical properties are evaluated by cyclic voltammetry and shown in Figure S2 and Table 1. The



**Figure 2.** Absorption spectra of 5,11- $\alpha\beta$ -TTN, 2,8- $\alpha\beta$ -TTN, and 4,9- $\alpha$ -aNDT, 4,9- $\beta$ -aNDT in dichloromethane at the concentration of ca.  $10^{-5}$  M.

**Table 1.** Molecular Properties of 5,11- $\alpha\beta$ -TTN and 2,8- $\alpha\beta$ -TTN

compound	HOMO (eV) <sup>a</sup>	LUMO (eV) <sup>b</sup>	$\lambda_{\text{max}}$ (nm) <sup>c</sup>	$E_g^{\text{opt}}$ (eV) <sup>d</sup>
5,11- $\alpha\beta$ TTN	−5.76	−2.51	296, 335, 350, 378	3.25
2,8- $\alpha\beta$ TTN	−5.70	−2.47	297, 338, 375	3.23

<sup>a</sup>Experimental values obtained by cyclic voltammetry. <sup>b</sup>LUMO energy level obtained by the equation: LUMO = HOMO +  $E_g^{\text{opt}}$ .

<sup>c</sup>Experimental values measured in the dichloromethane solution.

<sup>d</sup> $E_g^{\text{opt}} = 1240 / \lambda_{\text{onset}}$ .

HOMO energy levels of 5,11- $\alpha\beta$ -TTN and 2,8- $\alpha\beta$ -TTN were estimated to be −5.75 and −5.70 eV, respectively. DFT calculations were performed to elucidate the optical spectra and electronic properties of 5,11- $\alpha\beta$ -TTN and 2,8- $\alpha\beta$ -TTN with the Gaussian 09 suite at the MPW1PW91/6-311G-(d,p)/PCM=CH<sub>2</sub>Cl<sub>2</sub>//CAM-B3LYP/6-311G(d,p) level of theory. Dodecyl groups are all simplified with ethyl groups. For comparison, 4,9- $\alpha$ -aNDT and 4,9- $\beta$ -aNDT were computed as well. Calculated HOMO/LUMO energy, excitation energy, oscillator strength, and configuration of the excited states are listed in Table S2. Calculated molecular frontier orbital (plots, isovalue = 0.02 au) contours are depicted in Figure 3.

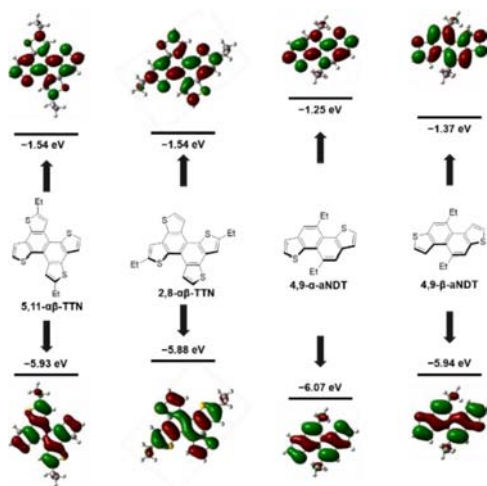


**Figure 3.** Calculated molecular frontier orbitals (plots, isovalue = 0.02 au) and corresponding energies (eV) for 5,11- $\alpha\beta$ -TTN, 2,8- $\alpha\beta$ -TTN, 4,9- $\alpha$ -aNDT, and 4,9- $\beta$ -aNDT.

Figure S3 includes computational fitting for experimental UV-vis spectra of 5,11- $\alpha\beta$ -TTN, 2,8- $\alpha\beta$ -TTN, 4,9- $\alpha$ -aNDT, and 4,9- $\beta$ -aNDT. As can be concluded from Table S2 and Figure S3, although there is slight deviation in the absolute values, the calculated estimations still correlate well with the experimental data, suggesting that the selected model of theory is appropriate for the studied molecules in this work.

As can be seen from Figure 3, 5,11- $\alpha\beta$ -TTN and 2,8- $\alpha\beta$ -TTN both have a more extended conjugated region than the 4,9- $\alpha$ -aNDT and 4,9- $\beta$ -aNDT, resulting in the higher HOMO and lower LUMO values and narrower energy band gaps. The X-ray single crystal structure of 5,11- $\alpha\beta$ -TTN is shown in Figure 4.

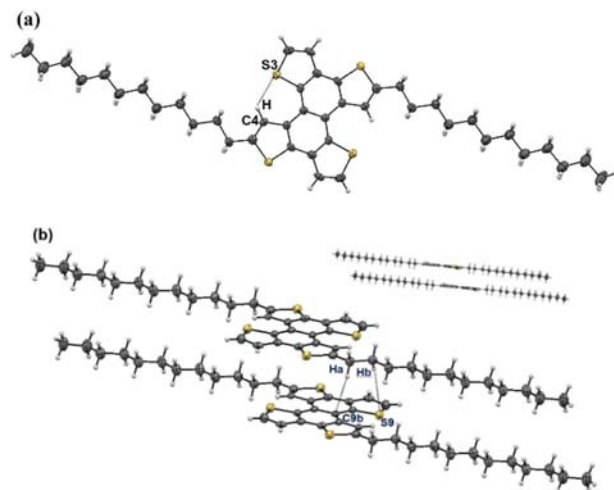
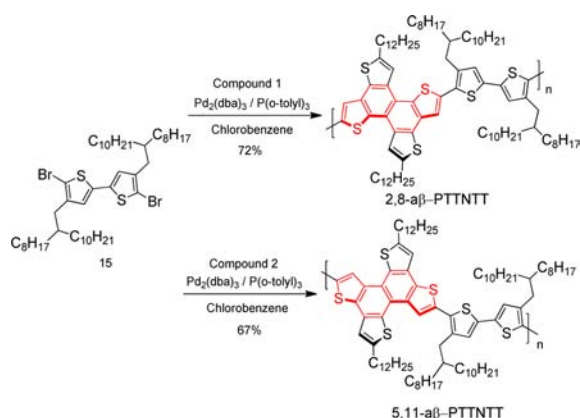


**Figure 4.** Top (a) and side view (b) of ORTEP: 5,11- $\alpha\beta$ -TTN (80% probability for thermal ellipsoids).

5,11- $\alpha\beta$ -TTN exhibited a highly planar 2-D conjugated structure. Intramolecular six-membered C—H...S hydrogen bonding might be present between the C<sup>4</sup>—H (C<sup>10</sup>—H) and S<sup>3</sup> (S<sup>9</sup>) in the fjord region. Natural Bond Orbital (NBO, CAM-B3LYP/6-311G-(d,p)) analysis was implemented to investigate this interaction existing in 5,11- $\alpha\beta$ -TTN (Figure S4). The energy was estimated to be 0.93 kcal mol<sup>−1</sup> due to the interaction between the sulfur's lone pair and the C—H anti-bonding orbital. The two didodecyl carbon chains are horizontally within the conjugation plane which might result from a number of intermolecular interactions between C<sup>9b</sup>/H<sub>a</sub> and S<sup>9</sup>/H<sub>b</sub>. A certain degree of  $\pi$ — $\pi$  stacking with a distance ca. 3.39 Å is also observed. Compounds 1 and 2 were polymerized with a 5,5'-dibromo-2,2'-bithiophene-based monomer (15) to obtain the two corresponding isomeric copolymers denoted as 2,8- $\alpha\beta$ -PTTNTT and 5,11- $\alpha\beta$ -PTTNTT, respectively (Scheme 4). The molecular characteristics of the two polymers are shown in Figures S7–S10. Organic field-effect transistors (OFETs) were fabricated with the bottom-gate/bottom-contact geometry to evaluate the mobility of the 2,8- $\alpha\beta$ -PTTNTT and 5,11- $\alpha\beta$ -PTTNTT. The OFETs using SiO<sub>2</sub> as a gate dielectric were treated with octadecyltrichlorosilane (ODTS) to form a self-assembly monolayer (SAM). The hole mobility was deduced from the transfer characteristics of the devices in the saturation regime (Figure S11). 2,8- $\alpha\beta$ -PTTNTT with the  $\alpha$ -aNDT moiety in the main chain exhibited a higher hole mobility of  $1.26 \times 10^{-2}$  cm<sup>2</sup> V<sup>−1</sup> s<sup>−1</sup> than 5,11- $\alpha\beta$ -PTTNTT ( $2.40 \times 10^{-4}$  cm<sup>2</sup> V<sup>−1</sup> s<sup>−1</sup>) using the  $\beta$ -aNDT segment in the polymer backbone. This result might be attributed to the more



**Scheme 4. Synthesis of 2,8- $\alpha\beta$ -PTTNTT and 5,11- $\alpha\beta$ -PTTNTT Copolymers**



linear main-chain curvature of 2,8- $\alpha\beta$ -PTTNTT, resulting in higher molecular ordering in the solid state.<sup>8</sup>

In summary, for the first time, we have designed and synthesized isomeric 5,11-didodecyl  $\alpha\beta$ -TTN and 2,8-didodecyl  $\alpha\beta$ -TTN. The didodecyl  $\alpha\beta$ -TTN molecules feature sufficient solubility, enhanced absorption ability, and high coplanarity. The corresponding 2,8-distannyl 5,11-didodecyl  $\alpha\beta$ -TTN (**1**) and 2,8-didodecyl 5,11-distannyl  $\alpha\beta$ -TTN (**2**) were polymerized with the bithiophene-based monomer to yield 2,8- $\alpha\beta$ -PTTNTT and 5,11- $\alpha\beta$ -PTTNTT copolymers. The isomeric conjugated structures play a pivotal role in determining the OFET mobility. 2,8- $\alpha\beta$ -PTTNTT with a more linear polymer backbone exhibited higher hole mobility. The synthesis and utilization of versatile  $\alpha\beta$ -TTN-based materials are currently underway in our laboratory.

## ■ ASSOCIATED CONTENT

### Supporting Information

The Supporting Information is available free of charge on the ACS Publications website at DOI: 10.1021/acs.orglett.5b03294.

X-ray crystallography, cyclic voltammograms, computational details, experimental procedures, characterization of two polymers, and <sup>1</sup>H and <sup>13</sup>C NMR spectra (PDF)

Crystallographic data for **6** (CIF)

Crystallographic data for 2,8-TIPS- $\alpha\beta$ -TTN (CIF)

## ■ AUTHOR INFORMATION

### Corresponding Author

\*E-mail: yjcheng@mail.nctu.edu.tw.

### Author Contributions

†S.-L.C. and C.-W.L. contributed equally.

### Notes

The authors declare no competing financial interest.

## ■ ACKNOWLEDGMENTS

We thank the Ministry of Science and Technology and the Ministry of Education, and Center for Interdisciplinary Science (CIS) of the National Chiao Tung University, Taiwan, for financial support. We thank the National Center of High-performance Computing (NCHC) in Taiwan for computer time and facilities. We thank Prof. Sue-Lein Wang at National Tsing Hua University (NTHU) for help with the X-ray crystallography.

Y.J.C. thanks the support from the Golden-Jade fellowship of the Kenda Foundation.

## ■ REFERENCES

- (a) Takimiya, K.; Shinamura, S.; Osaka, I.; Miyazaki, E. *Adv. Mater.* **2011**, *23*, 4347–4370. (b) Anthony, J. E. *Angew. Chem., Int. Ed.* **2008**, *47*, 452–483. (c) Wu, J.-S.; Cheng, S.-W.; Cheng, Y.-J.; Hsu, C.-S. *Chem. Soc. Rev.* **2015**, *44*, 1113–1154. (d) Cheng, Y.-J.; Yang, S.-H.; Hsu, C.-S. *Chem. Rev.* **2009**, *109*, 5868–5923.
- (a) Chen, Y. L.; Chang, C. Y.; Cheng, Y. J.; Hsu, C. S. *Chem. Mater.* **2012**, *24*, 3964–3971. (b) Huo, L. J.; Hou, J. H.; Zhang, S. Q.; Chen, H. Y.; Yang, Y. *Angew. Chem., Int. Ed.* **2010**, *49*, 1500–1503. (c) Liang, Y. Y.; Xu, Z.; Xia, J. B.; Tsai, S. T.; Wu, Y.; Li, G.; Ray, C.; Yu, L. P. *Adv. Mater.* **2010**, *22*, E135–E138 and 7595–7597.
- (a) Lehnher, D.; Waterloo, A. R.; Goetz, K. P.; Payne, M. M.; Hampel, F.; Anthony, J. E.; Jurchescu, O. D.; Tykewski, R. R. *Org. Lett.* **2012**, *14*, 3660–3663. (b) Mamada, M.; Minamiki, T.; Katagiri, H.; Tokito, S. *Org. Lett.* **2012**, *14*, 4062–4065. (c) Wu, J.-S.; Lin, C.-T.; Wang, C.-L.; Cheng, Y.-J.; Hsu, C.-S. *Chem. Mater.* **2012**, *24*, 2391–2399.
- (a) Osaka, I.; Abe, T.; Shinamura, S.; Takimiya, K. *J. Am. Chem. Soc.* **2011**, *133*, 6852–6860. (b) Shinamura, S.; Osaka, I.; Miyazaki, E.; Nakao, A.; Yamagishi, M.; Takeya, J.; Takimiya, K. *J. Am. Chem. Soc.* **2011**, *133*, 5024–5035.
- (a) Loser, S.; Bruns, C. J.; Miyauchi, H.; Ortiz, R. P.; Facchetti, A.; Stupp, S. I.; Marks, T. J. *J. Am. Chem. Soc.* **2011**, *133*, 8142–8145. (b) Shinamura, S.; Sugimoto, R.; Yanai, N.; Takemura, N.; Kashiki, T.; Osaka, I.; Miyazaki, E.; Takimiya, K. *Org. Lett.* **2012**, *14*, 4718–4721. (c) Nakano, M.; Shinamura, S.; Sugimoto, R.; Osaka, I.; Miyazaki, E.; Takimiya, K. *Org. Lett.* **2012**, *14*, 5448–5451.
- Cheng, S. W.; Chiou, D. Y.; Lai, Y. Y.; Yu, R. H.; Lee, C. H.; Cheng, Y. J. *Org. Lett.* **2013**, *15*, 5338–5341.
- Osaka, I.; Houchin, Y.; Yamashita, M.; Kakara, T.; Takemura, N.; Koganezawa, T.; Takimiya, K. *Macromolecules* **2014**, *47*, 3502–3510.
- (a) Osaka, I.; Kakara, T.; Takemura, N.; Koganezawa, T.; Takimiya, K. *J. Am. Chem. Soc.* **2013**, *135*, 8834–8837. (b) Cheng, S. W.; Tsai, C. E.; Liang, W. W.; Chen, Y. L.; Cao, F. Y.; Hsu, C. S.; Cheng, Y. J. *Macromolecules* **2015**, *48*, 2030–2038. (c) Cheng, S.-W.; Chiou, D.-Y.; Tsai, C.-E.; Liang, W.-W.; Hsu, C.-Y.; Lai, Y.-Y.; Hsu, C.-S.; Osaka, I.; Takimiya, K.; Cheng, Y.-J. *Adv. Funct. Mater.* **2015**, *25*, 6131–6143.
- (a) He, F.; Wang, W.; Chen, W.; Xu, T.; Darling, S. B.; Strzal-ka, J.; Liu, Y.; Yu, L. *J. Am. Chem. Soc.* **2011**, *133*, 3284–3287. (b) Min, J.; Zhang, Z. G.; Zhang, S. Y.; Li, Y. F. *Chem. Mater.* **2012**, *24*, 3247–3254.
- (a) Peng, Q.; Liu, X. J.; Su, D.; Fu, G. W.; Xu, J.; Dai, L. M. *Adv. Mater.* **2011**, *23*, 4554–4558. (b) Liu, B.; Chen, X. W.; He, Y. H.; Li, Y. F.; Xu, X. J.; Xiao, L.; Li, L. D.; Zou, Y. P. *J. Mater. Chem. A* **2013**, *1*, 570–577. (c) Zhang, M. J.; Gu, Y.; Guo, X.; Liu, F.; Zhang, S. Q.; Huo, L. J.; Russell, T. P.; Hou, J. H. *Adv. Mater.* **2013**, *25*, 4944–4949. (d) Wang, M.; Hu, X.; Liu, P.; Li, W.; Gong, X.; Huang, F.; Cao, Y. *J. Am. Chem. Soc.* **2011**, *133*, 9638–9641.
- (a) Fischer, E.; Larsen, J.; Christensen, J. B.; Fourmigue, M.; Madsen, H. G.; Harrit, N. J. *J. Org. Chem.* **1996**, *61*, 6997–7005. (b) Wang, Z.; Shi, J.; Wang, J.; Li, C.; Tian, X.; Cheng, Y.; Wang, H. *Org. Lett.* **2010**, *12*, 456–459. (c) Dou, C. D.; Saito, S.; Gao, L. B.; Matsumoto, N.; Karasawa, T.; Zhang, H. Y.; Fukazawa, A.; Yamaguchi, S. *Org. Lett.* **2013**, *15*, 80–83. (d) Song, J. S.; Wu, T. J.; Zhao, X. Q.; Kan, Y. H.; Wang, H. *Tetrahedron* **2015**, *71*, 1838–1843.
- (a) Yamamoto, A.; Ohta, E.; Kishigami, N.; Tsukahara, N.; To-miyori, Y.; Sato, H.; Matsui, Y.; Kano, Y.; Mizuno, K.; Ikeda, H. *Tetrahedron Lett.* **2013**, *54*, 4049–4053.
- Dou, C. D.; Saito, S.; Gao, L. B.; Matsumoto, N.; Karasawa, T.; Zhang, H. Y.; Fukazawa, A.; Yamaguchi, S. *Org. Lett.* **2013**, *15*, 80–83.
- Fürstner, A.; Mamane, V. *J. Org. Chem.* **2002**, *67*, 6264–6267.
- (a) Zhai, L.; Shukla, R.; Wadumethrige, S. H.; Rathore, R. J. *Org. Chem.* **2010**, *75*, 4748–4760. (b) Zhai, L.; Shukla, R.; Rathore, R. *Org. Lett.* **2009**, *11*, 3474–3477. (c) Waghray, D.; de Vet, C.; Karypidou, K.; Dehaen, W. *J. Org. Chem.* **2013**, *78*, 11147–11155.